ELSEVIER

Physica A 263 (1999) 405–414

PHYSICA A

Slow dynamics and regularization phenomena in ensembles of chaotic neurons

M. I. Rabinovich [a 1], P. Varona [a,b], J. J. Torres [a], R. Huerta [a,b] and H. D. I. Abarbanel [a,c]

[a] *Institute for Nonlinear Science. UCSD, 9500 Gilman Dr., La Jolla, Ca, 92093-0402.*

[b] *GNB. Dpto. de Ing. Informática. ETSI. UAM, Cantoblanco. 28049 Madrid.*

[c] *Dept. of Physics and Marine Physical Laboratory, Scripps Institution of Oceanography. UCSD.*

Abstract

We have explored the role of calcium concentration dynamics in the generation of chaos and in the regularization of the bursting oscillations using a minimal neural circuit of two coupled model neurons. In regions of the control parameter space where the slowest component, namely the calcium concentration in the endoplasmic reticulum, weakly depends on the other variables, this model is analogous to three dimensional systems as found in [1] or [2]. These are minimal models that describe the fundamental characteristics of the chaotic spiking-bursting behavior observed in real neurons. We have investigated different regimes of cooperative behavior in large assemblies of such units using lattices of non-identical Hindmarsh-Rose neurons electrically coupled with parameters chosen randomly inside the chaotic region. We study the regularization mechanisms in large assemblies and the development of several spatio-temporal patterns as a function of the interconnectivity among nearest neighbors.

PACS: 05.45.+b; 47.52.+j; 87.22.Jb; 07.05.Mh

Keywords: Chaotic spiking-bursting neurons; Regularization mechanisms; Spatio-temporal patterns; Coarse grain dynamics.

1 Introduction

How detailed should a model of a central pattern generator (CPG) describing, say, locomotion of an animal be? Must it describe, based on genetic information, the protein composition of the membrane and numerous features of the neuromodulators responsible for the activity of ion channels of the cell in order to have a biologically justified model of a neuron and a CPG as a whole? Should one take into account details of the spikes propagating through axons and their transformation into chemical signals in synapses? Of course, it would be desirable to take all these factors into consideration. A CPG model constructed in this fashion would, in principle, explain and predict the dependence of rhythmic activity on any parameters, e. g., on the change of ambient temperature. It

[1] Corresponding author. Phone (619) 534-6753. Fax: (619) 534-7664. Email: mrabinovich@ucsd.edu

0378-4371/99/$ – see front matter
PII: S0378-4371(98)00528-7

seems clear that it is presently impossible to construct such a detailed model: ion channels are numerous, couplings among neurons are sometimes ambiguous, and the neurons are different as a rule. In addition, the rich architecture of neural circuits and the diversified characteristic time scales determining dynamic activity of constituent elements make a direct attack very difficult. What can one rely upon in such a situation? We believe there are two interesting directions: (i) the detailed investigation of the simplest circuits within the framework of realistic models of neurons and synapses justified biologically [3], and (ii) construction of phenomenological models of complex neural circuits consisting of large assemblies of simple model neurons [4]. In an ideal case, a combination of these two ways should give rather effective, structurally stable (in the sense of the theory of dynamic systems) models of neural circuits that take into account both information about elementary acts of coupling among real neurons and key cooperative effects.

In this research we attempt to apply aspects of each of these approaches to neural circuits consisting of spiking-bursting chaotic neurons. In particular, we investigate the mechanisms of synchronization and regularization of neural network dynamics for (i) a system of two coupled neurons, and (ii) a large lattice of different chaotic neurons. A detailed model of spiking-bursting chaotic neurons is used for a minimal circuit, with primary attention focused on the role of slow $[Ca^{2+}]$ dynamics as it affects the processes of synchronization and regularization. A three-dimensional model of spiking-bursting chaotic neurons is used for the lattice simulations. There we focus on the spatio-temporal patterns observed in the cooperative behavior and on the analysis of the averaged behavior of a group of neurons (coarse grain dynamics).

2 Synchronization and Regularization Phenomena in Two Coupled Chaotic Neurons. The Role of Endoplasmic Reticular Ca^{2+} Dynamics.

Based on experimental observations [5,6], we have built a two-compartment model of the lobster's stomatogastric LP neuron [3] to study chaotic and synchronization phenomena observed in the stomatogastric CPG. The model incorporates six active ionic currents distributed in two compartments (soma-neuropil and axon) depending on their slow/fast evolution (see figure 1). A detailed calcium dynamics for the soma compartment includes Ca^{2+} storage in the endoplasmic reticulum and Ca^{2+} diffusion through the luminal and through the cytoplasmic membrane. Recent studies indicate that the presence of calcium oscillations inside the endoplasmic reticulum has significant effects in the cytoplasmic membrane potential oscillations [7–10]. Our simulations show that the slow calcium concentration dynamics inside the endoplasmic reticulum ($[Ca^{2+}]_{er}$) may have an important role in generating and regulating the chaotic bursting-spiking activity of these neurons. The concentration of inositol 1,4,5-triphosphate (IP_3) receptor appears as a control parameter in this model.

A complete description of the currents (conductance variables described by Hodgkin-Huxley and Goldman-Hodgkin-Katz formalisms) and the calcium dynamics for the single neuron model can be found in [3]. For all the simulations described in this paper, the IP_3 concentration was set at the regime where the neurons fire chaotic bursts. We have reproduced four sets of experiments carried out using the dynamic clamp technique which

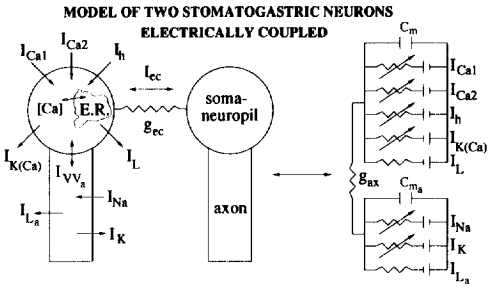

Fig. 1. Schematic description of the model of two stomatogastric LP neurons coupled electrically. The model includes a detailed characterization of the $[Ca^{2+}]$ storage and diffusion in the endoplasmic reticulum of each neuron. f_1, f_2 and f_3 stand for complex dependencies on their arguments and on other biophysical parameters such as pumping rates, buffering coefficients and activation and inactivation variables.

allows us to change the conductance of the electrical coupling between two real neurons (the conductance associated with the electrical coupling between these type of neurons is $g_{ec} \approx 0.100 - 0.200\mu S$ in the natural state). Depending on the strength of the coupling, different collective behaviors are observed: from independent chaotic bursting to synchronized chaotic bursting and to anti-phase regular activity.

When the two model neurons are coupled with null or small coupling conductance ($g_{ec} \approx 0.001\mu S$) independent chaotic behavior is observed (see [3] for a detailed characterization of the chaos in the single neuron model). Membrane potential bursts range from half a second to two seconds without periodicity (see figure 2a). The number of spikes on the top of the slow waves also changes from burst to burst. Note that local maxima of cytoplasmic calcium concentration ($[Ca^{2+}]$) mark the end of the burst plateaus. Calcium concentration inside the endoplasmic reticulum ($[Ca^{2+}]_{ER}$) evolves slowly modulating (in anti-phase) the faster oscillations of cytoplasmic $[Ca^{2+}]$ and influencing on the length of the voltage plateaus. We will discuss the evolution of these three variables for different coupling strengths g_{ec}.

A moderate value ($g_{ec} \approx 0.05\mu S$) for the coupling conductance between the two model neurons causes burst (slow wave) synchronization but not spike synchronization (see figure 2b and also $V_1(t)$ vs. $V_2(t)$ plot in figure 3b). This synchronization of the slow waves is the observed behavior for two real stomatogastric neurons interacting with their natural electrical coupling. Note that, in our simulations for this conductivity range, $[Ca^{2+}]$ and $[Ca^{2+}]_{ER}$ oscillate in a similar fashion for both neurons but they are not completely in phase, in spite of the existing burst synchronization for the membrane potential.

Whenever the two model neurons are coupled with a high electrical conductance, $g_{ec} > 0.2\mu S$, complete synchronization both for slow waves and fast action potentials is observed, see figure 2c and also $V_1(t)$ vs. $V_2(t)$ plot for the membrane potentials in figure 3c. Note that $[Ca^{2+}]$ and $[Ca^{2+}]_{ER}$ now oscillate more in phase between the two neurons than in the previous cases, but yet their trajectories do not overlap.

For all three cases discussed so far, small, medium and high positive coupling conductance, the bursting activity remains irregular regardless of the degree of synchronization.

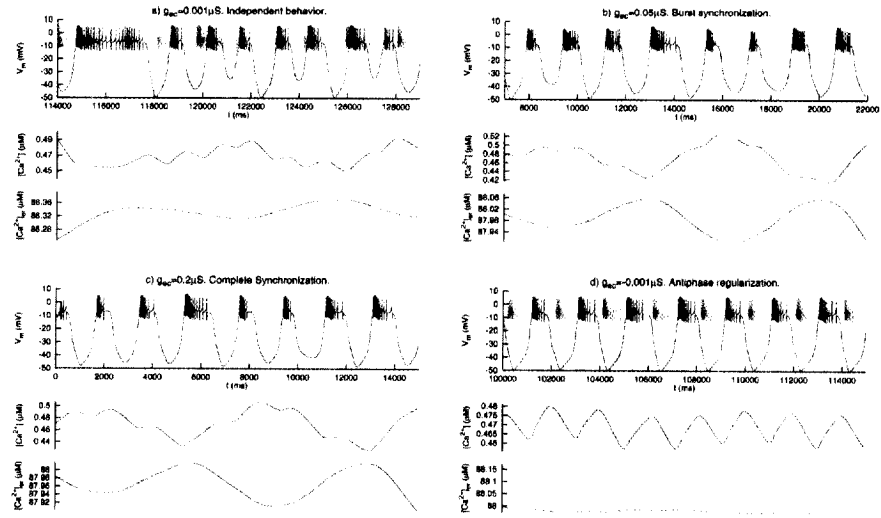

Fig. 2. Four different collective behaviors observed when two LP model neurons are coupled electrically (cf. figure 2 in [5]): a) independent chaotic bursting activity, b) burst synchronization, c) total synchronization and d) anti-phase synchronization with regularization. Activity for neuron one is plotted with a dark trace; neuron two is represented with a light trace. In each of the graphs, from top to bottom: membrane potential V_m, cytoplasmic calcium concentration ($[Ca^{2+}]$), and calcium concentration inside the endoplasmic reticulum ($[Ca^{2+}]_{ER}$).

Thus, synchronization occurs without regularization. When the two neurons are coupled with a small negative conductance $g_{ec} = -0.001\mu S$, thus inverting the sign of the current coming from the electrical coupling in both neurons, anti-phase synchronization is observed in the membrane potentials, see figure 2d. Furthermore, the two neurons regulate their bursting behavior in the sense that the lengths of the burst are kept uniform. As can be noted in figure 2d, $[Ca^{2+}]_{ER}$ remains nearly constant for the two neurons, while $[Ca^{2+}]$ oscillates regularly but in anti-phase with respect to the other neuron. Note than in the previous cases $[Ca^{2+}]_{ER}$ oscillated slowly with a large amplitude. In our model, chaotic behavior is sustained in the single neuron model whenever $[Ca^{2+}]_{ER}$ oscillations are present. If $[Ca^{2+}]_{ER}$ is kept constant, the model produces regular bursting activity. For a small negative electrical coupling, the calcium dynamics in the ER of each neuron is maintained constant, since the fast oscillations of calcium in the cytoplasm are rapid enough and regular enough to have no influence on the slower calcium diffusion through the endoplasmic reticulum membrane. Again, once the calcium concentration in the ER is kept constant, regularization of the chaotic behavior occurs. This behavior is also observed when the regularization is obtained by periodic driving through small periodic pulses of current injection and when the two neurons are coupled with mutual inhibitory chemical synapses.

All four cases of synchronization observed in the experiments with electrically coupled real neurons and reproduced here using our model are summarized in figure 3. This figure displays $V_1(t)$, the membrane voltage in neuron 1, against $V_2(t)$ in neuron 2 and shows

the synchronization status for both slow and fast oscillations depending on the value of the electrical coupling conductance g_{ec} between the two neurons. g_{ec} is the only model parameter changed in these four simulations.

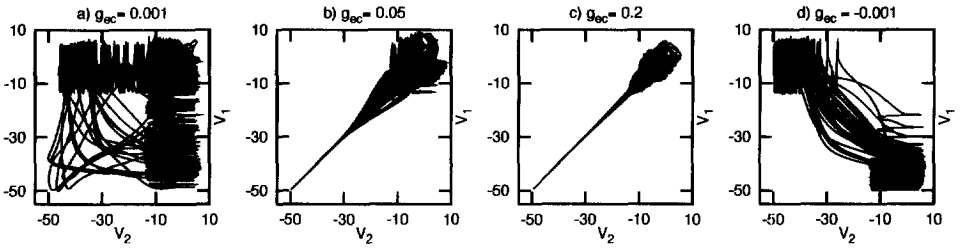

Fig. 3. Portraits of membrane potential V_1 vs. V_2 showing the synchronization phenomena between the two neurons for all four cases discussed previously: a) independent bursting activity, b) slow wave synchronization, c) total synchronization and d) anti-phase regularization.

The modeling of small lattices of LP two-compartment neurons with electric couplings among nearest neighbors show that this regularization mechanism induced by the slow dynamics of $[Ca^{2+}]_{ER}$ is also robust when the neurons are coupled to more than one neighbor.

3 Pattern formation with anti-phase regularization

As we discussed in the previous section, a pair of electrically coupled chaotic neurons with mutual negative conductance behave regularly in the regime of anti-phase bursting oscillations. Using a detailed model of a stomatogastric neuron, we have pointed out the role that the slow calcium dynamics may have in the origin of this regularization. Now we turn from the analysis of the dynamical origin of the regularization in a system of two neurons to the study of the collective behavior in large assemblies of electrically coupled neurons that have similar slow dynamics involved in the generation of their spiking-bursting behavior. In order to make feasible the simulation of large lattices of neurons, here we use the Hindmarsh-Rose (H-R) three dimensional system [2] to model each neuron. This model reproduces the basic characteristics of the chaotic spiking-bursting behavior observed in CPG neurons.

We have built a network of non-identical H-R neurons with parameters selected randomly in the regime of chaotic oscillations [11]. Each model neuron is connected to its nearest neighbors through an electrical coupling. The dynamics is described by the following system of equations:

$$\frac{dx_{i,j}}{dt} = y_{i,j} + 3x_{i,j}^2 - x_{i,j}^3 - z_{i,j} + I_{i,j} - g_{ec} \sum_{(l,m)\in\Lambda} (x_{i,j} - x_{l,m}) \tag{1}$$

$$\frac{dy_{i,j}}{dt} = 1 - 5x_{i,j}^2 - y_{i,j} \tag{2}$$

$$\frac{dz_{i,j}}{dt} = -rz_{i,j} + rS(x_{i,j} + 1.6) \tag{3}$$

where $i, j = 1 \ldots N$ indicate location on the two dimensional $N \times N$ lattice Λ and l, m indexes run over the four nearest neighbors of each unit (i, j). The parameters used for all the simulations described in this paper are: $I_{i,j} = 3.281 \pm 0.05$, $r = 0.0021$ and $S = 4$. Here, g_{ec} is the strength of the electrical coupling, a parameter analogous to the coupling conductance used in the LP model neurons of the previous section. As in our previously discussed model of the stomatogastric CPG, the dynamics of the H-R model is also characterized by two different time scales. Here, we are abstracting this behavior using just two fast dynamical variables and a slow one. The subsystem of $(x_{i,j}, y_{i,j})$ in the H-R model is responsible for the fast oscillations or the spiking activity, and the slow subsystem is represented by $z_{i,j}$. The fast subsystem is placed in the state space near a homoclinic bifurcation and, along with the slow subsystem, generates chaotic oscillations.

As in the biophysical model presented in section 2, anti-phase synchronization is observed when a negative value for g_{ec} is used in equation 1. We have studied the formation of different patterns of activity in the background of these alternating anti-phase oscillations depending on the size of the network. For small networks (typically in the order of 10 by 10 neurons) total anti-phase synchronization and regularization is observed among nearest neighbors (see figure 4a, top). We will use the following order parameter $a(t)$ to measure the evolution of the activity of the network Λ:

$$a(t) = \frac{1}{2}\left[\frac{1}{N_{\Lambda_A}} \sum_{(i,j)\in\Lambda_A} x_{i,j}(t) - \frac{1}{N_{\Lambda_B}} \sum_{(i,j)\in\Lambda_B} x_{i,j}(t)\right] \tag{4}$$

where Λ_A and Λ_B represent two interconnected sublattices (chess board configuration) such that a neuron located in Λ_A has all its nearest neighbors in Λ_B, and vice versa ($\Lambda_A \cup \Lambda_B = \Lambda$ and $\Lambda_A \cap \Lambda_B = \emptyset$). N_{Λ_A} and N_{Λ_B} are the number of units in each sublattice. In figure 4a, dark squares represent the neurons in the subnetwork Λ_A with low activity (sub-threshold) and white squares represent the neurons in the subnetwork Λ_B with high activity (above threshold). The order parameter $a(t)$ is plotted as a function of time at the bottom of each column in figure 4.

Figure 4b shows a snapshot of the network for a medium (30 by 30) lattice of H-R networks coupled with negative conductances for a time step when a transition from sub-threshold to supra-threshold activity occurs. Although not noticeable in the scale used to plot $a(t)$ in figure 4b, this transition is slower than the one in the previous case. This allows to distinguish the wave shown in figure 4b whenever the transition takes place. Figure 4c shows a snapshot of the network activity for a large network composed of 50 by 50 neurons. In this case, well defined waves of state transition separate domains of anti-phase behavior. The waves are periodic in time over the whole network. This effect can be understood looking at the behavior of $a(t)$. If, as in this case, the network is big enough the change from sub-threshold to supra-threshold activity takes place in a time scale much greater than the previous cases. Furthermore, the system does not stay in any of these states for a long time and this induces the formation of the spatio-temporal

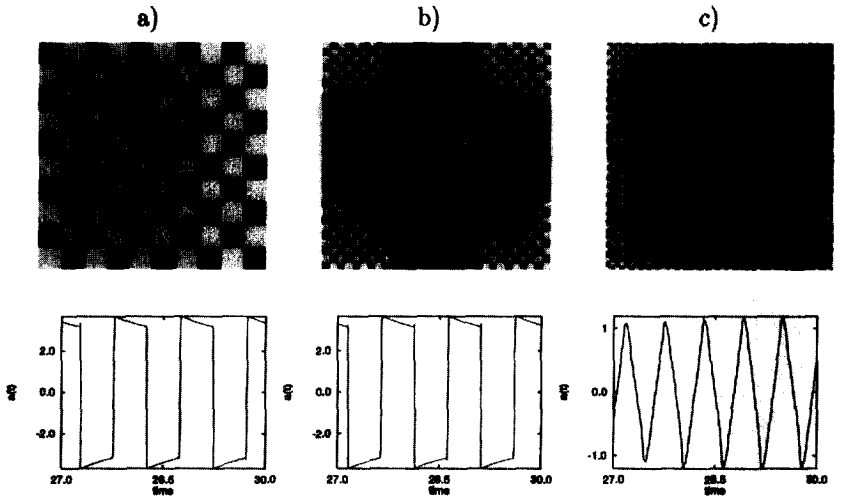

Fig. 4. Patterns of anti-phase synchronous behavior for three networks of H-R neurons electrically coupled with negative conductance ($g_{ec} = -1.12$): a) network of 10 by 10 neurons, b) network of 30 by 30 neurons, c) network of 50 by 50 neurons. At the bottom of each column the order parameter $a(t)$ is plotted as a function of time.

patterns.

4 Pattern formation and regularization on "coarse-grain" lattices

We have also built networks of H-R neurons with positive values for g_{ec} in equation 1. In this case, the choice for the sign correspond to natural diffusive electrical coupling among nearest neighbors. We found three main regimes of synchronization depending on the strength of the electrical coupling g_{ec}: spiking (complete), partial (clustering) and bursting synchronization. Regularization of the slow wave is observed for all these cases. The average activity $< x(t) >= 1/N^2 \sum_{i,j=1}^{N} x_{i,j}(t)$ can be used to study the global behavior of the lattice and to identify the temporal characteristics, particularly, to distinguish among the different types of global synchronization. When there is no synchronization, the average activity remains very close to a constant value. When the average activity is periodic and nearly constant at the top of the bursts, the system is in bursting synchronization. When there is complete synchronization, the behavior of any individual unit is identical to the average activity of the whole lattice.

In spite of the heterogeneity and chaotic behavior of the individual elements, lattices of spiking-bursting neurons coupled diffusively show striking spatio-temporal patterns: clusters of synchronization and regularization of the slow dynamics as seen in figure 5. The boundaries of the clusters are the fronts of phase triggering between in-phase and out of phase synchronization. These contrast patterns reproduce themselves periodically in time. This regime coexists in control parameter space within the regime of bursting

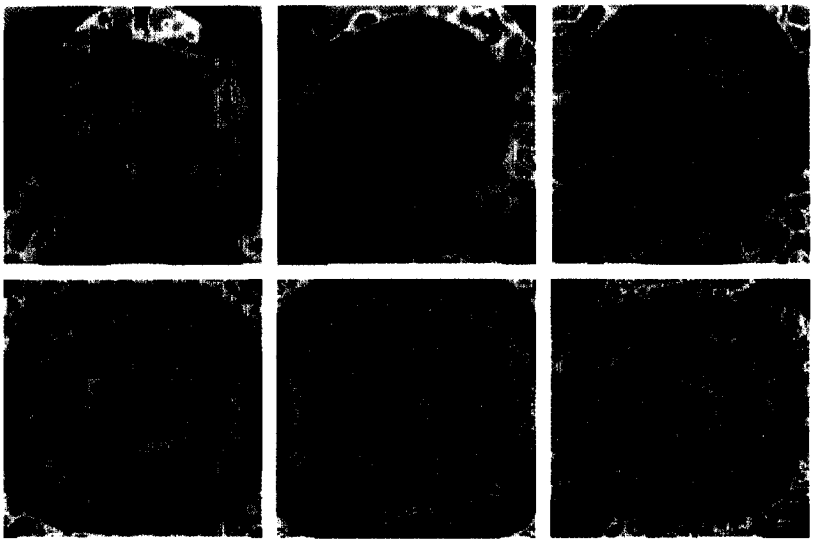

Fig. 5. Evolution of partial synchronization patterns in a network of 100x100 H-R neurons coupled electrically with positive conductance.

synchronization that is homogeneous in space and periodic in time (bistability).

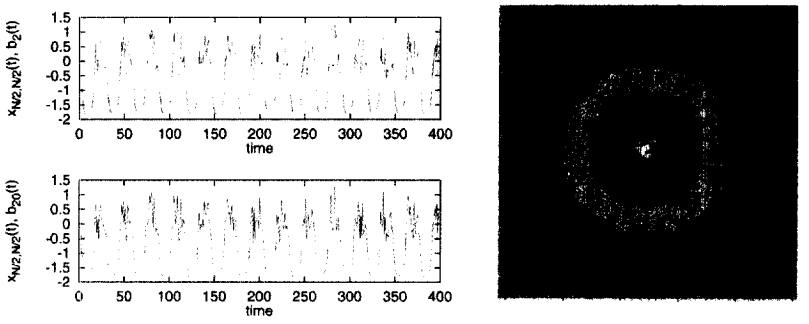

Fig. 6. Evolution of coarse grain dynamics in the network shown in figure 5 ($g_{ec} = 1.5$). Top: $x_{N/2,N/2}$, the activity of the neuron located at the center of the cluster, is shown (dark trace) together with the average activity of the cluster $b_R(t)$ for a radius $R = 2$ (light trace). Bottom: same figure for $R = 20$. In this simulation $g_{ec} = 1.5$. Right, degree of synchronization for different radii of the cluster. See text for further explanation.

The dependence in R for the degree of synchronization between the activity in the center of the cluster and the average activity in the cluster ($g_e = 1.5$) is shown in figure 6.

We define its value as $(1-\sigma_R)\times 100$, where

$$\sigma_R^2 = \frac{1}{T}\int_{t_0}^{t_0+T} dt\left[x_{N/2,N/2}(t) - b_R(t)\right]^2. \tag{5}$$

where $b_R(t)$ is the average activity of a cluster centered at $(N/2, N/2)$: $b_R(t) = \frac{1}{N_{\Lambda_C}}\sum_{(i,j)\in\Lambda_C} x_{i,j}(t)$, and $\Lambda_C = \{(i,j) : (i-\frac{N}{2})^2 + (j-\frac{N}{2})^2 \leq R^2, i,j = 1\ldots N\}$. This measure reveals the presence of coarse grain phenomena in the activity of such networks.

The collective dynamics of chaotic neurons with local interactions often exhibit "non-trivial" cooperative behavior exhibiting a rich variety of phase transitions. Such behavior is "non-trivial" because the chaotic dynamics of these lattices with short-scale interaction shows extensive chaos: the number of Lyapunov exponents increases with the size of the lattice. Actually, the cooperative behavior of chaotic lattices depends strongly on the strength of the local connection, and this reveals a rich diversity of levels of synchronization in the coarse grain phenomena.

5 Discussion

In this paper we have used two different models to study the collective behavior of chaotic spiking-bursting neurons. The first model was a minimal network composed of two biologically plausible neurons coupled electrically. Using this detailed model we reproduced experimental results that show how the irregular bursting behavior in the stomatogastric neurons can turn to regular when the coupling conductance is changed. We have also pointed out the role of the slow calcium dynamics in the endoplasmic reticulum as the main variable that leads the chaotic dynamics in this model. Whenever the interaction between the two neurons makes $[Ca^{2+}]_{ER}$ dynamics nearly constant (e.g. when fast $[Ca^{2+}]_{cyt}$ oscillations are present in anti-phase behavior), the bursting activity becomes regular.

We have built several networks of H-R neurons coupled electrically with negative and positive conductances to study the behavior of large lattices of chaotic bursting neurons. The size of the network influences on the collective behavior and on the development of spatio-temporal patterns of activity. We investigated here two different mechanisms involved in the regularization phenomena of ensembles of spiking-bursting chaotic neurons. The first mechanism is related to the stability of anti-phase behavior of two coupled neurons, which is provided by either mutual synaptic inhibition or negative electrical coupling. The homoclinic nature of the fast oscillations are regulated by the slow oscillations. The value of the slow variable increases as the model neuron is spiking. If there is no inhibition to cut the raise of this slow variable, the system will be driven near the homoclinic bifurcation, which is structurally unstable. Mutual inhibition, either by negative electrical coupling (or synaptic coupling), will avoid that the neuron reaches the structurally unstable fast oscillations. The second mechanism of regularization (for diffusive coupling) is related to the synchronization of the slow bursting behavior of individual neurons by periodic averaged field. Such bind of the regularization is only possible for large lattices

so that the coarse grain can emerge. The slow dynamics of such course grain is periodic and it seems reasonable to build simplify versions of the model in the parameter regions of interest by considering the lattice of coarse grain units with regular dynamics.

Acknowledgments

This work has been supported by grants from ORD (H. D. I. A.), DOE (H. D. I. A., M. I. R), MEC (P. V.) and Universidad de Granada (J. J. T.).

References

[1] T. R. Chay. Biological Cybernetics 75 (1996) 419.
[2] J. L. Hindmarsh and R. M. Rose. Proc R. Soc. Lond. B 221, (1984) 87.
[3] M. Falcke, R. Huerta, M.I. Rabinovich, H.D.I. Abarbanel, R. Elson, A. Selverston. Preprint.
[4] M. Bazhenov, R. Huerta, M. I. Rabinovich, T. Sejnowski. Physica D 1858 (1998) 1.
[5] R. Elson, A.I. Selverston, R. Huerta, N. F. Rulkov, M.I. Rabinovich, H.D.I. Abarbanel, to be published in Physical Review Letters.
[6] R. Elson, P. Varona, J.J. Torres, M.I. Rabinovich, H.D.I. Abarbanel. Soc. Neurosci. Abstr 655.8 (1998).
[7] M. J. Berridge. Neuron. 21 (1998) 13.
[8] X-Y. Li, J. Keizer, S.S. Stojilkovic, J. Rinzel. Am. J. Physiol. 269 (1995) (5 Pt 1) C1079.
[9] Y-X Li, J. Rinzel, S.S. Stojilkovic. Biophysical Journal. 69 (1995) 785.
[10] Y-X Li, S.S. Stojilkovic, J. Keizer, J. Rinzel. Biophysical Journal 72 (1997) 1080.
[11] R. Huerta, H. Bazhenov, M.I. Rabinovich, Europhys. Lett. 43 (6) (1998) 719-724.